INTERNATIONAL JOURNAL OF ENERGY STUDIES

e-ISSN: 2717-7513 (ONLINE); homepage: https://dergipark.org.tr/en/pub/ijes

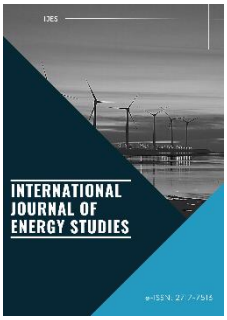

Research Article
Int J Energy Studies 2025; 10(3): 699-710
DOI: 10.58559/ijes.1697104

Received : 11 May 2025
Revised : 06 July 2025
Accepted : 08 July 2025

Determination of optimum Cu/(Ga+In) ratio at different fabrication temperatures for Cu(In,Ga)(Se,Te)$_2$ thin film solar cells

Semih Ağca[a*], Güven Çankaya[b]

[a]*Department of Metallurgical and Materials Engineering, Faculty of Engineering and Natural Sciences, Ankara Yıldırım Beyazıt University, Ankara, 06010, Türkiye, ORCID: 0000-0002-4834-5337*

[b]*Department of Metallurgical and Materials Engineering, Faculty of Engineering and Natural Sciences, Ankara Yıldırım Beyazıt University, Ankara, 06010, Türkiye, ORCID: 0000-0003-2932-1695*

*(*Corresponding Author:semihagca@aybu.edu.tr)*

Highlights

- Optimum CGI values for 480°C and 620°C substrate temperatures were found to be 0.88 and 0.90, respectively.
- The sample with 0.90 CGI ratio which produced at 620°C performed the best efficiency with 14.23 %.
- The CGI ratio affected the the short circuit current and fill factor more than the open circuit voltage.

You can cite this article as: Ağca S, Çankaya G. Determination of optimum Cu/(Ga+In) ratio at different fabrication temperatures for Cu(In,Ga)(Se,Te)$_2$ thin film solar cells. Int J Energy Studies 2025; 10(3): 699-710.

ABSTRACT

In this study, tellurium-dopped Cu(In,Ga)(Se,Te)$_2$ completed solar cells with different Cu/(Ga+In) ratios were fabricated at different substrate temperatures and investigated to understand the effect of Cu/(Ga+In) ratio on the solar parameters and the structure of the solar cells. It was found that the Cu/(Ga+In) ratio affected the short circuit current and fill factor more than the open circuit voltage by changing the microstructure. Therefore, the increase in the current collection and short circuit current density had a greater effect on the efficiency value. Increasing the Cu/(Ga+In) ratio from 0.88 to 0.90 decreased the average grain size from 0.47 µm to 0.38 µm at 480°C substrate temperature. However, further increasing the Cu/(Ga+In) ratio from 0.90 to 0.92 made the structure more compact having an average grain size of 0.41 µm with less thin film quality. The samples with highest Cu/(Ga+In) ratios having the most compact structures in their temperature groups showed very low current collection through all wavelengths when compared to other samples. The short circuit current density results were found to be in consistency with the external quantum efficiency graphs of the completed solar cell samples. Optimum Cu/(Ga+In) values for the samples produced at 480°C and 620°C substrate temperatures were found to be 0.88 and 0.90, respectively. The sample with 0.90 CGI ratio which produced at 620°C performed the best efficiency with 14.23 %.

Keywords: Solar cell, Thin film, Tellurium, CGI ratio

1. INTRODUCTION

Thin film solar cells, which can adapt to different application conditions in space and on earth, have the potential to solve many problems in safe and sustainable energy supply. The radiation resistance of these solar cells, their ability to be produced flexibly and to absorb light very well with a very thin structure bring important advantages such as lightness, foldability and long-term durability in space conditions. On the other hand, being produced transparently can offer solutions such as more effective use of agricultural lands and aesthetic exterior cladding for buildings instead of glass in earth conditions [1-5].

Copper indium gallium selenide (CIGS) solar cells constitute an important group of thin film solar cells with their chalcopyrite structure and properties such as tunable direct bandgap, low material usage, high absorption coefficient, long term stability, and high efficiency [6-12]. The chalcogen component in the calcopyrite structures of these solar cells can be S, Se, Te, or a mixture of these elements. By altering the chalcogen, it is possible to adjust the bandgap value of the thin film solar cell and improve the thin film quality [13-21].

In order to produce highly efficient thin film CIGS solar cells, the chemical composition of the absorber layer, which is one of the most important layers in electricity generation, must be adjusted very precisely. It has been stated in the literature that Cu/(Ga+In) (CGI) and Ga/(Ga+In) (GGI) ratios are important indicators of chemical composition [22]. The effects of gallium amount and GGI ratio on solar cell parameters in tellurium-doped CIGS thin film solar cells have been included in our previous studies [14, 15]. However, to the best of our knowledge, the effect of CGI ratio on the structure and solar cell parameters in tellurium-doped CIGS solar cells has not yet been reported in the literature.

In this study, complete Te-dopped CIGS solar cells with different CGI ratios were fabricated at different substrate temperatures and investigated to understand the effect of CGI ratio on the solar parameters and the structure of the solar cells.

2. EXPERIMENTAL DETAILS

The substrate material for solar cell fabrication was obtained from Nice Solar Energy GmbH as soda lime glass plates having 400 nm thick molybdenum back contact coating. These plates were cut to inch by inch dimensions by mechanical scribing, cleaned by potassium hydroxide solution

for 10 minutes, and dried by dry nitrogen before absorber layer deposition. The absorber layers of the solar cells were deposited on these Mo-coated soda lime glasses with three-stage co-evaporation method at 480°C and 620°C substrate temperatures by a multi-source physical vapor deposition chamber. The substrate temperatures were chosen as the highest temperature that the SLG glass can withstand without deformation and the lowest temperature at which the diffusion mechanisms can operate properly and high efficiency values can be achieved according to the literature [13-15]. By not using a diffusion barrier layer, the sodium in the soda lime glass was able to reach the absorber layer. In addition, in order for the sodium amount to reach a sufficient amount, post-deposition treatment was applied by depositing 6 nm thick NaF on the 2 μm thick absorber layer.

Se-Te mixture chalcogen was used by adding 0.1 atomic percent tellurium to the structure. The GGI ratios of the solar cells were kept constant at 0.25. The production parameters were set such that the CGI ratios of the solar cells produced at both temperatures were 0.88, 0.90, and 0.92. The selected CGI ratios were chosen to understand how small changes in the 0.90 CGI ratio, which produces the best CIGS solar cells, will affect the efficiency [22]. Samples are named as 4-88, 4-90, 4-92, 6-88, 6-90, and 6-92 with the left side of the dash representing the production temperature and the right side representing the CGI ratio. For example, sample named 4-90 was produced with a substrate temperature of 480°C and a CGI ratio of 0.90. The CdS buffer layer, which is the n-type component of the p-n junction, was deposited with chemical bath deposition method. Magnetron sputtering was used for ZnO and ITO coatings. The aluminum front contact, which was coated with double-sided nickel, was deposited by e-beam evaporation. The thicknesses of CdS, ZnO, ITO, Al and Ni were 50 nm, 100 nm, 200 nm, 2 μm, and 30 nm, respectively. The active area of each solar cells was roughly 0.5 cm^2.

The SEM microstructure photos were taken by ZEISS Supra 40VP SEM with a 5kV acceleration voltage. The chemical compositions of the samples were determined by a Bruker EDS with an acceleration voltage of 15 kV. The solar cell parameters of open circuit voltage (V_{OC}), short circuit current density (J_{SC}), fill factor (FF), and the power conversion efficiency (PCE) were obtained by using J-V measurement method with a four-point measurement setup. The current collection behaviour of the solar cells were examined by an external quantum efficiency (EQE) setup having a xenon lamp and equipped with a monochromator. J-V and EQE measurements were carried out under AM1.5G standard test conditions at room temperature.

3. RESULTS AND DISCUSSION

The SEM microstructure photos of the samples just after the absorber layer deposition and the post-deposition treatment are shown in Figure 1.

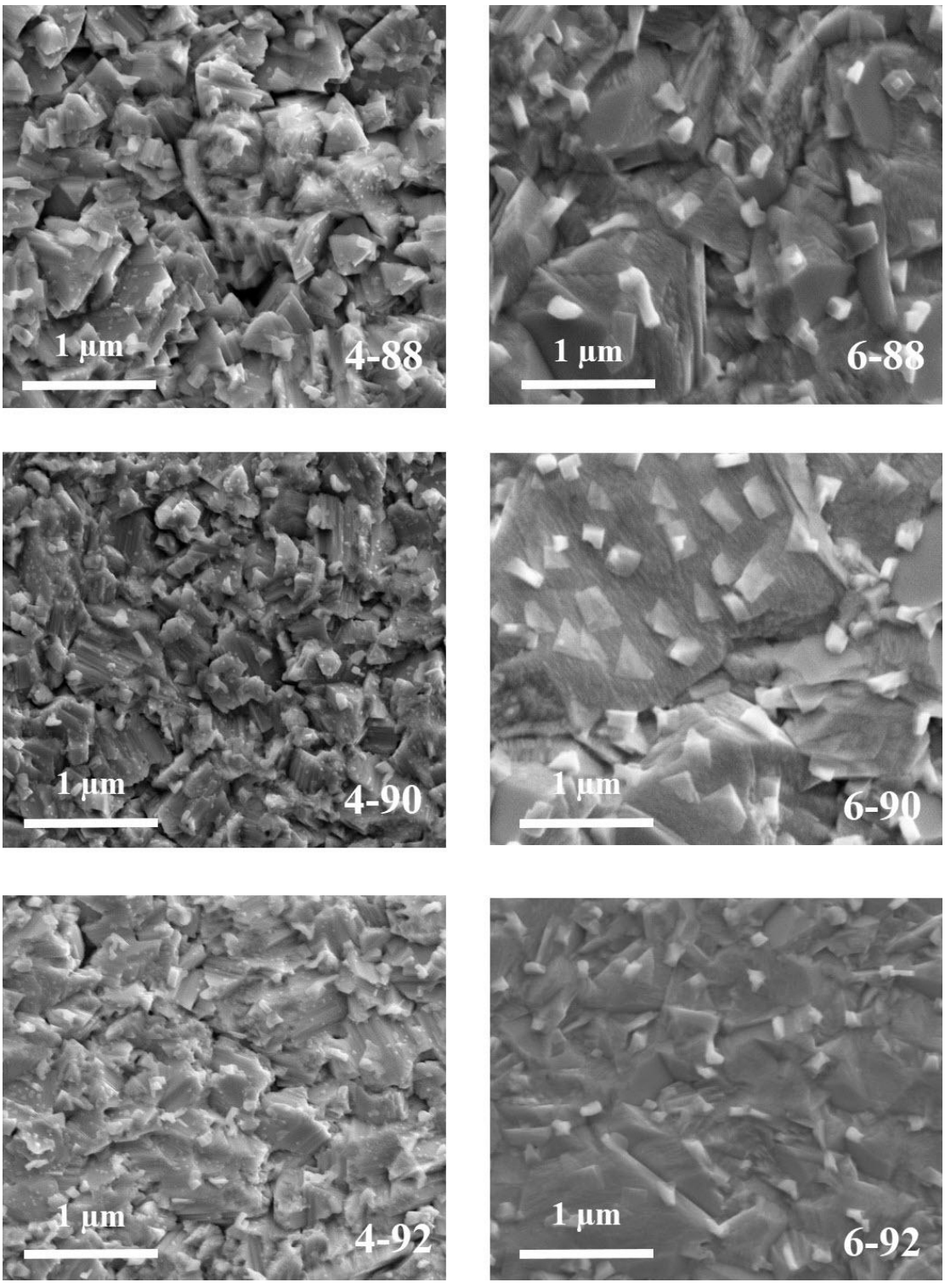

Figure 1. The SEM microstructure photos of the samples just after the absorber layer deposition and the post-deposition treatment

It can be seen from Figure 1 that the samples produced at higher temperature have larger grains when compared to the samples produced at lower temperatures. Since the production times of all samples were nearly equal, the temperature component of the diffusion mechanism played a crucial role and affected the nucleation and growth dynamics.

To understand the effect of CGI ratio on the grain structure, the samples produced at the same temperature can be compared. Increasing the CGI ratio from 0.88 to 0.90 decreased the average grain size from 0.47 μm to 0.38 μm at 480°C substrate temperature. However, further increasing the CGI from 0.90 to 0.92 made the structure more compact with an average grain size of 0.41 μm. When all samples produced at 480°C substrate temperature are considered, it is seen that the sample with the highest CGI ratio have the most compact structure.

Copper has the highest melting point among the components in the CIGS structure. There may have been a slight decrease in the melting point of the CIGS compound due to less copper in the structure. Therefore, the liquid phase assisted crystallization mechanism, which is not normally expected to be seen at these temperatures, may have worked to some extent, making the average grain size of 4-88 larger than that of 4-90 [20]. On the other hand, the reason behind the compact structure of the sample having the highest CGI ratio may be due to an expansion with the increasing trend in the $CuSe_2$ phase ratio with the increase in the copper amount [23]. It is observed that in all samples produced at 480°C substrate temperature, NaF particles (small white particles) were in the nm scale and were homogeneously distributed in the structure.

When the samples produced at 620°C substrate temperature were compared, sample 6-90 has the largest average grain size with 1.56 μm while the sample 6-92 has the most compact structure. The average grain sizes of samples 6-88 and 6-92 were found to be 0.84 μm and 0.65 μm, respectively. The fact that the samples produced at 620°C substrate temperature have larger average grain sizes than the samples produced at 480°C substrate temperature is quite consistent with the literature [13, 14, 24]. Increasing the substrate temperature decreased the nucleation cites of NaF particles by decreasing the surface roughness, thus the size of NaF particles increased to approximately 200 nm due to the high temperature and low number of nucleation cites.

The fact that the sample with the highest CGI ratio among the samples produced at 620°C substrate temperature has the most compact structure can be explained by the same mechanism in the samples produced at 480°C substrate temperature. On the other hand, the different alteration of average grain sizes of the samples may be due to the balance between the stoichiometry and the fabrication temperature. Consequently, the largest average grain size and the most compact structure were found to be in sample 6-90 and 6-92, respectively. The EQE graphs of the completed solar cell samples are shown in Figure 2.

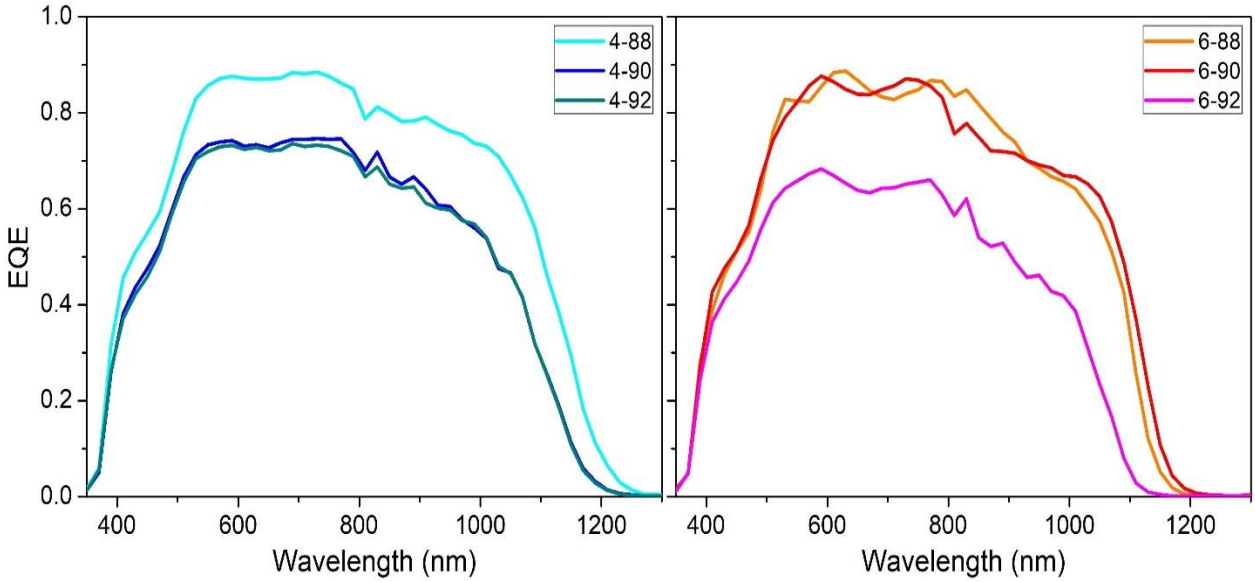

Figure 2. The EQE graphs of the completed solar cell samples

It can be clearly seen from Figure 2 that the samples 4-92 and 6-92 having the most compact structures in their temperature groups showed very low current collection through all wavelengths when compared to other samples. Being more compact may have increased sunlight reflectance, reducing the amount of light absorbed and thus reducing the current collection [25]. On the other hand, sample 4-90 also showed very low current collection without being compact. The lower average grain size may have caused a decrease in thin film quality, which in turn may have reduced the light path due to reflection, thus decreasing the probability of collection [26, 27].

The current collection of sample 6-88 was higher that that of sample 6-90 only between 800 nm and 900 nm wavelength. On the other wavelength regions, sample 6-90 showed a slightly higher current collection than the sample 6-88. Thus, sample 6-90 has the best current collection among

the samples prodeced at 620°C substrate temperature. However, when sample 4-88 is compared with 6-88 and 6-90 it can be seen that sample 4-88 has the best current collection among all samples especially with its higher collection on the wavelengths larger than 800 nm. The variation in the long-wavelength limits observed in the EQE graphs were thought to be due to the change in the bandgap of the samples with increasing copper concentration. The bandgap values of the samples 4-88, 4-90, 4-92, 6-88, 6-90, and 6-92 were derived from the normalized EQE data and were found to be 1.06 eV, 1.09 eV, 1.09 eV, 1.11 eV, 1.09 eV, and 1.15 eV, respectively. The J-V graphs of the completed solar cell samples are shown in Figure 3.

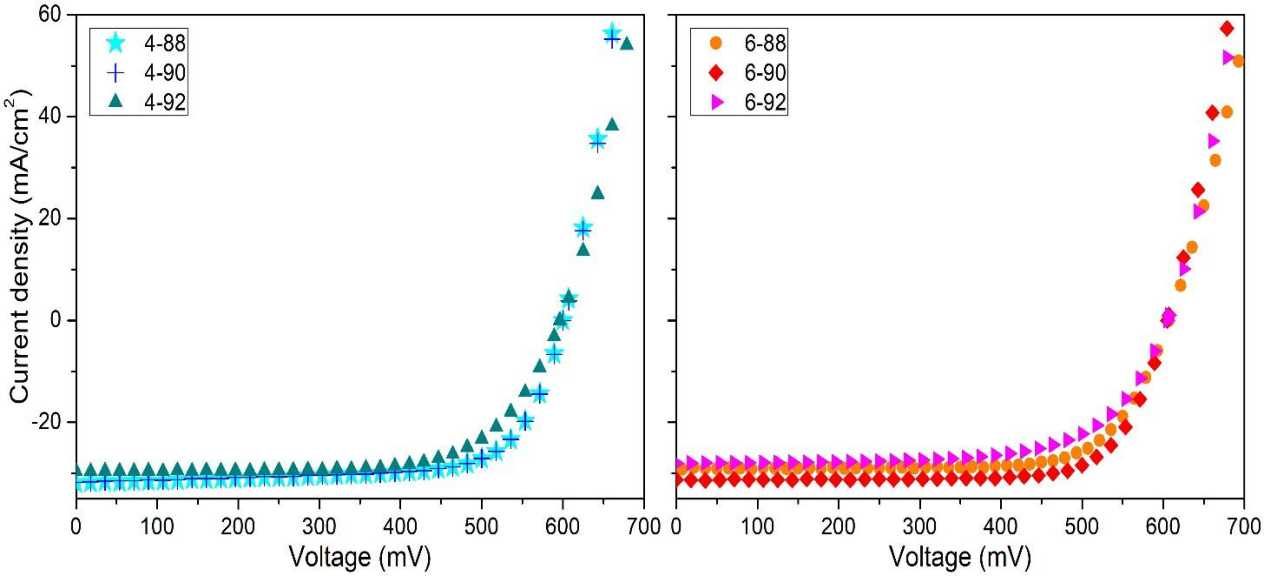

Figure 3. The J-V graphs of the completed solar cell samples

The solar cell parameters of the completed solar cell samples were derived from the J-V graphs and shown in Table 1.

Table 1. The solar cell parameters of the completed solar cell samples

Sample	V_{OC} (mV)	J_{SC} (mA/cm^2)	FF (%)	PCE (%)
4-88	600	31.9	70.8	13.56
4-90	600	31.7	71.0	13.52
4-92	596	29.6	69.0	12.16
6-88	607	29.2	72.7	12.89
6-90	605	31.3	75.2	14.23
6-92	605	28.0	66.8	11.33

The J_{SC} results were found to be in consistency with the EQE graphs of the completed solar cell samples. Therefore, the effect of CGI ratio and the substrate temperature on the J_{SC} values can be understood by the explanation in the EQE results section. J_{SC} values of the samples were also calculated by the integration of the EQE results with the AM1.5G solar spectrum to compare with the J_{SC} values derived from J-V results. The J_{SC}(EQE) values of samples 4-88, 4-90, 4-92, 6-88, 6-90, and 6-92 were found to be 33.67 mA/cm^2, 27.46 mA/cm^2, 27.02 mA/cm^2, 31.72 mA/cm^2, 31.75 mA/cm^2, and 22.79 mA/cm^2, respectively, and it was determined that these values followed the same trend as the J_{SC}(J-V) values. The V_{OC} values of the samples produced at 620°C substrate temperature were found to be higher than that of 480°C.

This may be due to larger grains, less grain boundaries, and less recombination occuring in grain boundaries [28]. The FF values of the samples having more compact structure but lower thin film quality were found to be less than other members of their temperature groups. This may be due to a disorder problem at the CIGS-CdS interface [29, 30]. When PCE values of the completed solar cell samples produced at 480°C substrate temperature were compared, it can be seen that the optimum CGI ratio for the best PCE was 0.88. On the other hand, the optimum CGI ratio was found to be 0.90 for the samples produced at 620°C. The sample 6-90 showed the best performance with a PCE of 14.23 %.

4. CONCLUSION

The determination of optimum CGI ratio at different substrate temperatures for CIGS thin film solar cells were investigated. It can be concluded that the increase in the CGI ratio from 0.88 to 0.90 decreased the average grain size from 0.47 µm to 0.38 µm at 480°C substrate temperature. However, further increasing the CGI from 0.90 to 0.92 made the structure more compact with an average grain size of 0.41 µm. When the samples produced at 620°C substrate temperature were compared, it is found that the sample 6-90 has the largest average grain size while the sample 6-92 has the most compact structure.

The samples 4-92 and 6-92 having the most compact structures in their temperature groups showed very low current collection through all wavelengths when compared to other samples. On the other hand, sample 4-90 also showed very low current collection without being compact. The current collection of sample 6-88 was higher that that of sample 6-90 only between 800 nm and 900 nm wavelength. On the other wavelength regions, sample 6-90 showed a slightly higher current collection than the sample 6-88. Thus, sample 6-90 has the best current collection among the

samples produced at 620℃ substrate temperature. However, when sample 4-88 is compared with 6-88 and 6-90 it can be seen that sample 4-88 has the best current collection among all samples especially with its higher collection on the wavelengths larger than 800 nm. Optimum CGI values for the samples produced at 480℃ and 620℃ substrate temperatures were found to be 0.88 and 0.90, respectively. The sample 6-90 had the best PCE with 14.23 %. In this study, only two different production temperatures were studied. Extensive and systematic studies are required to determine the optimum values of the CGI ratio at different production temperatures.

ACKNOWLEDGMENT

This study was supported by TÜBİTAK 2214-A and TÜBİTAK 2211-C Scholarship Programmes. We would like to thank to PV Group of Prof. Dr. Roland Scheer in the Physics Institute of Martin-Luther University Halle-Wittenberg for their support with the laboratory infrastructure.

DECLARATION OF ETHICAL STANDARDS

The authors of the paper submitted declare that nothing which is necessary for achieving the paper requires ethical committee and/or legal-special permissions.

CONTRIBUTION OF THE AUTHORS

Semih Ağca: Performing the experiments and analyzing the results, writing the manuscript.

Güven Çankaya: Bringing the idea, supervising the study, final check of the manuscript.

CONFLICT OF INTEREST

There is no conflict of interest in this study.

REFERENCES

[1] Minoura S, Kodera K, Maekawa T, Miyazaki K, Niki S, Fujiwara H. Dielectric function of Cu(In, Ga)Se2-based polycrystalline materials. Journal of Applied Physics 2013; 113: 063505.

[2] Bulbul S, Ertugrul G, Arli F. Investigation of usage potentials of global energy systems. International Advanced Researches and Engineering Journal 2018; 2: 58-67.

[3] Başol BM, Kapur VK, Leidholm CR, Halani A, Gledhill K. Flexible and lightweight copper indium diselenide solar cells on polyimide substrates. Solar Energy Materials and Solar Cells 1996; 43: 93-98.

[4] Conibeer GJ, Willoughby A. Solar cell materials: Developing technologies. John Wiley and Sons Ltd, England, 2014.
[5] Lee TD, Ebong AU. A review of thin film solar cell technologies and challenges. Renewable and Sustainable Energy Reviews 2017; 70: 1286-1297.
[6] Jäger-Waldau A. Status and perspectives of thin film photovoltaics - Thin film solar cells: Current status and future trends. Nova Science Publishers Inc, New York, US, 2010.
[7] Poortmans J, Arkhipov V. Thin film solar cells: Fabrication, characterization, and applications. John Wiley & Sons, West Sussex, England, 2006.
[8] Naghavi N, Mollica F, Goffard J, Posada J, Duchatelet A, Jubault M, Donsanti F, Cattoni A, Collin S, Grand PP, Greffet JJ, Lincot D. Ultrathin Cu(In,Ga)Se2 based solar cells. Thin Solid Films 2017; 633: 55-60.
[9] Sun Y, Lin S, Li W, Cheng S, Zhang Y, Liu Y, Liu W. Review on alkali element doping in Cu(In,Ga)Se2 thin films and solar cells. Engineering 2017; 3: 452-459.
[10] Fiat S, Bacaksiz E, Kompitsas M, Çankaya G. Temperature and tellurium (Te) dependence of electrical characterization and surface properties for a chalcopyrite structured schottky barrier diode. Journal of Alloys and Compounds 2014; 585: 178-184.
[11] Fiat S, Koralli P, Bacaksiz E, Giannakopoulos KP, Kompitsas M, Manolakos DE, Çankaya G. The influence of stoichiometry and annealing temperature on the properties of CuIn0.7Ga0.3Se2 and CuIn0.7Ga0.3Te2 thin films. Thin Solid Films 2013; 545: 64-70.
[12] Dumrul H, Arlı F, Taşkesen E. Dust Effect on PV Modules: Its Cleaning Methods. Innovative Research in Engineering 2023; 183-200.
[13] Ağca S, Çankaya G. Photovoltaic properties of Cu(In,Ga)(Se,Te)2 thin film solar cells with different tellurium amounts and a copper-poor stoichiometry. International Journal of Energy Studies 2023; 8(4): 849-858.
[14] Ağca S, Çankaya G. Effect of gallium content on diode characteristics and solar cell parameters of Cu(In1-xGax)(Se0.98Te0.02)2 thin film solar cells produced by three-stage co-evaporation at low temperature. Gazi University Journal of Science Part C: Design and Technology 2023; 11(4): 1108-1115.
[15] Ağca S, Çankaya G, Sonmezoglu S. Impact of tellurium as an anion dopant on the photovoltaic performance of wide-bandgap Cu(In,Ga)Se2 thin-film solar cells with rubidium fluoride post-deposition treatment. Frontiers in Energy Research 2023; 11: 1215712.
[16] Fiat S, Polat I, Bacaksiz E, Çankaya G, Koralli P, Manolakos DE, Kompitsas M. Optical and structural properties of nanostructured CuIn0.7Ga0.3(Se(1−x)Tex)2 chalcopyrite thin films—

Effect of stoichiometry and annealing. Journal of Nanoscience and Nanotechnology 2014; 14: 5002-5010.

[17] Varol SF, Bacaksiz E, Koralli P, Kompitsas M, Çankaya G. A novel nanostructured CuIn0.7Ga0.3(Se0.4Te0.6)2/SLG multinary compounds thin films: For photovoltaic applications. Materials Letters 2015; 142: 273-276.

[18] Fiat S, Polat İ, Bacaksiz E, Kompitsas M, Çankaya G. The influence of annealing temperature and tellurium (Te) on electrical and dielectrical properties of Al/p-CIGSeTe/Mo Schottky diodes. Current Applied Physics 2013; 13: 1112-1118.

[19] Varol SF, Bacaksız E, Çankaya G, Kompitsas M. Optical, structural, and morphological characterization of CuIn0.7Ga0.3(Se0.6Te0.4)2 thin films under different annealing temperatures. Celal Bayar University Journal of Science 2013; 9: 9-16.

[20] Atasoy Y, Başol B, Olğar M, Tomakin M, Bacaksız E. Cu(In,Ga)(Se,Te)2 films formed on metal foil substrates by a two-stage process employing electrodeposition and evaporation. Thin Solid Films 2018; 649: 30-37.

[21] Atasoy Y, Başol B, Polat İ, Tomakin M, Parlak M, Bacaksız E. Cu(In,Ga)(Se,Te)2 pentenary thin films formed by reaction of precursor layers. Thin Solid Films 2015; 592: 189-194.

[22] Kodigala SR. Cu(In1-xGax)Se2 Based Thin Film Solar Cells. Massachusetts: Academic Press, USA, 2011.

[23] Thompson JO, Anderson MD, Ngai T, Allen T, Johnson DC. Nucleation and growth kinetics of co-deposited copper and selenium precursors to form metastable copper selenides. Journal of Alloys and Compounds 2011; 509: 9631-9637.

[24] Liao KH, Su CY, Ding YT, Koo HS. Microstructural characterization of CIGS formation using different selenization processes. Applied Surface Science 2013; 270: 139-144.

[25] Scholtz L, Ladanyi L, Mullerova J. Influence of surface roughness on optical characteristics of multilayer solar cells. Advances in Electrical and Electronic Engineering 2015; 12: 631-638.

[26] Singh R, Parashar M, Sandhu S, Yoo K, Lee JJ. The effects of crystal structure on the photovoltaic performance of perovskite solar cells under ambient indoor illumination. Solar Energy 2021; 220: 43-50.

[27] Saive R. Light trapping in thin silicon solar cells: A review on fundamentals and technologies. Progress in Photovoltaics: Research and Applications 2021; 29:1125-1137.

[28] Gloeckler M, Sites JR, Metzger WK. Grain-boundary recombination in Cu(In,Ga)Se2 solar cells. Journal of Applied Physics 2005; 98: 113704.

[29] Guirdjebaye N, Ngoupo AT, Ouedraogo S, Tcheum GLM, Ndjaka JMB. Numerical analysis of CdS-CIGS interface configuration on the performances of Cu(In,Ga)Se2 solar cells. Chinese Journal of Physics 2020; 67: 230-237.

[30] Chen SH, Lin WT, Chan SH, Tseng SZ, Kuo CC, Hu SC, Peng WH, Lu YT. Photoluminescence analysis of CdS/CIGS interfaces in CIGS solar cells. ECS Journal of Solid State Science and Technology 2015; 4: 347-350.